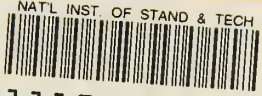


~~A11100 995221~~

NBS
PUBLICATIONS

NATL INST. OF STAND & TECH

A11106 979100

NBSIR 81-1648

INTERIM PROGRESS REPORT:

J-INTEGRAL METHOD FOR FITNESS-FOR-SERVICE ASSESSMENT

D.T. Read
H.I. McHenry

Fracture and Deformation Division
National Measurement Laboratory
National Bureau of Standards
Boulder, Colorado 80303

Sponsored by:
David Taylor Naval Ship Research & Development Center
Annapolis, MD 21402

May 1981

QC
100
.U56
81-1648
1981
c. 2

NBSIR 81-1648

e 17

INTERIM PROGRESS REPORT:

J-INTEGRAL METHOD FOR FITNESS-FOR-SERVICE ASSESSMENT

D.T. Read

H.I. McHenry

Fracture and Deformation Division
National Measurement Laboratory
National Bureau of Standards
Boulder, Colorado 80303

May 1981

Sponsored by:

David Taylor Naval Ship Research & Development Center
Annapolis, MD 21402



U.S. DEPARTMENT OF COMMERCE, Malcolm Baldrige, Secretary

NATIONAL BUREAU OF STANDARDS, Ernest Ambler, Director

Interim Progress Report:
J-integral Method for Fitness-for-Service Assessment

D. T. Read* and H. I. McHenry*

National Bureau of Standards
Boulder, Colorado 80303

Progress to date on the J-integral fitness-for-service assessment project is reported. The goal of this project is to produce a method for evaluation of material toughness requirements, allowable defect sizes, and sustainable stresses and strains. Yielding fracture mechanics and, specifically, the J-integral are employed. The J-integral is regarded as the crack driving force; applied J values above some critical value are predictive of material tearing. The applied J value is a function of applied stress and strain, crack length, and material tensile properties. The critical J-integral value is measured in material fracture-toughness tests. The experimental focus of the present study is on measurement of the applied J-integral as a function of stress and strain in HY130 specimens with different crack lengths. Neither experimental data nor established predictive theories for the behavior of applied J values are available in the literature for short cracks, the type most likely to be found in a structural element. Results for relatively large cracks indicate that displacements imposed at the specimen ends are transmitted in full to the cracked cross section. The displacements add to the strain field of the crack and produce a large applied J value. This behavior is described as net section yielding. For relatively short cracks, displacements imposed at the specimen ends are absorbed as plastic strain all along the specimen length, add only slightly to the strain field of the crack, and produce small applied J values. This behavior is described as gross section yielding. It is important to note that cracks as small as 5% of the total cross section have been found to exhibit net section yielding.

Key Words: Crack opening displacement; design curve; elastic-plastic fracture mechanics; fitness-for-service; fracture mechanics; J-integral.

*Fracture and Deformation Division, National Measurement Laboratory

ADMINISTRATIVE INFORMATION

This report was prepared as part of the Fracture Control Technology Program under the sponsorship of Dr. H. H. Vanderveldt, Naval Sea Systems Command (SEA 05R15). The effort was monitored by Mr. John P. Gudas, David Taylor Naval Ship Research and Development Center, Code 2814, under Program Element 627IN, Task Area SF 61-544-504.

INTRODUCTION

In 1978, the Naval Sea Systems Command started a program entitled "Fracture Control Technology for Ships and Submarines." The initial tasks included the identification of Navy fracture control requirements [1]¹ and an assessment of fracture control practices used by United States [2] and foreign [3] industries. The review of Navy requirements identified several questions that advances in fracture control technology may help to answer:

1. How much toughness is sufficient for a given application?
2. How large a defect can be tolerated in a given structural element, particularly in welds and castings?
3. How can one take the results of a fracture toughness test and apply them to a complex structural configuration?
4. How can elastic plastic fracture mechanics be reduced to a form useful to the Navy?

The assessments of fracture control practices revealed a technical approach that may serve as a useful pattern for the development of a method to answer these questions: fitness-for-service evaluation based on the crack-opening-displacement (COD) design curve [4]. This approach has been widely used, particularly in Europe, to answer similar questions for a variety of structural applications [5].

The key ingredient of a fitness-for-service assessment methodology is an elastic-plastic-fracture-mechanics relationship between applied strain, flaw size, and required toughness. Given such a relationship, one can proceed to answer the questions cited earlier. Minimum toughness

¹ Numbers in brackets indicate the literature references at the end of the paper.

requirements can be based on conservative estimates of the anticipated service stress and strain levels and flaw sizes. Allowable defect sizes and associated repair decisions can be based on specified toughness levels and maximum credible stress levels. Conceptually speaking, elastic-plastic-fracture mechanics could be readily applied to a wide range of complex structures in a manner analogous to the way linear-elastic-fracture mechanics (LEFM) is applied to aircraft structures.

The purpose of this program is to develop a fitness-for-service approach that would be applicable to the high-strength, high-toughness alloys used by the Navy. The specific objectives are:

1. To develop experimental methods to relate required toughness, flaw size, and applied strain under elastic-plastic loading conditions;
2. To relate required toughness to applied strain experimentally for a variety of flaw sizes and configurations in specimens that simulate structural elements;
3. To develop analytical methods that are reliable predictors of the experimental results and, implicitly, of structural behavior;
4. To demonstrate the validity of such methods by using wide plate tests on HY130 weldments.

The present report is the first interim report on the continuing program to accomplish these objectives; the experimental methods and experimental results for single-edge-notched tensile panels are described. This report consists of a discussion of the technical approach and a

brief summary of the experimental procedures and results. The two appendices are technical publications in which the experimental procedures and the results for a C-Mn ship steel and for HY130 steel are presented in detail.

TECHNICAL APPROACH

The technical approach is modeled after the COD design curve developed by the British Welding Institute [4]. There are, however, two fundamental differences in this approach: the J-contour integral, J, is used as the fracture criterion instead of the COD, and the experimental methods of developing the relationship of the required toughness to strain and flaw size are completely different. In this section, the COD-design-curve approach is reviewed and the J-integral approach is introduced and described.

The COD Design Curve

The COD design curve relates required fracture toughness, δ_c , applied strain, ϵ , and allowable flaw size, a , as shown in figure 1. The curve is an empirical lower bound derived from the results of wide plate tests. A given data point (x,y) used to derive the curve consists of (1) an x-coordinate of ϵ/ϵ_y , where ϵ is the failure strain in the wide-plate test and ϵ_y is the yield strain of the test material, and (2) a y-coordinate of $\delta_c/2\pi\epsilon_y\bar{a}$, where δ_c is the COD fracture toughness measured with a full-thickness bend test on the same material used in the wide-plate test and \bar{a} is the effective defect size parameter for the crack in the wide plate test. Thus, a given data point requires a fracture-toughness test and a wide-plate test.

The COD design curve is used to make fitness-for-service assessments in cases where two of the three variables -- δ_c , ϵ , and \bar{a} -- can be

safely estimated. From the design curve, the third variable is assessed, e.g., minimum toughness requirements can be established if ϵ and \bar{a} are given, etc. The parameters ϵ and \bar{a} are defined to permit assessment of a wide range of conditions. The effective defect size parameter, a is the half-length of an equivalent through-thickness crack. The design is used in accordance with rules for calculating a for a range of defect types including surface defects, embedded defects, clustered defects, and defects adjacent to fillets or holes. The applied strain, ϵ , is the sum of the average membrane strain, bending strain, residual strain, and peak strain due to a local stress concentration.

The COD design curve is useful in its present form to evaluate fitness-for-service for a wide range of structures and materials [5]. However, it is not developed sufficiently for use in critical Naval applications. The underlying empirical data base does not include enough results on the high-strength, high-toughness alloys used in Naval vessels and many of the underlying assumptions have not been critically evaluated, e.g., the calculation of \bar{a} for a surface flaw, the treatment of stress concentrations and residual stresses, and the assumption of uniform strain after yielding. To overcome these shortcomings, it was decided to use the COD design curve as the model for the development of a method for fitness-for-service assessment using materials of interest to the Navy.

The J-integral Approach

Given the task of developing a fitness-for-service assessment methodology for the Navy, the first consideration was selection of a

fracture criterion. The J-contour integral described by Rice [6] had two critical attributes: first, it had been used as an elastic-plastic fracture criterion [7,8,9]; second, it had been measured as a function of strain in single specimens in configurations different from standard fracture-toughness specimens [10,11,12]. It was not considered feasible to measure COD as a function of strain for nonstandard specimen geometries. No well-developed elastic-plastic-fracture-mechanics fracture criterion other than J or COD was available. Therefore, the J-contour integral was selected as the fracture criterion for use in a fitness-for-service assessment method patterned on the COD-design-curve approach.

The needed relationship of the required J-integral fracture toughness to applied strain and flaw size was derived by assuming that the required material toughness at a given strain level and defect size was simply equal to the J contour integral measured at that strain level and defect size. This was seen as a natural extension of the assumption used in J-integral fracture-toughness testing that the applied J contour integral at crack initiation is taken as the material fracture toughness. In defect size assessment, the largest acceptable defect size would be the size at which the J contour integral was equal to the material fracture toughness. Similarly, the largest acceptable strain level would be the level for which the applied J for the defect size under consideration was equal to the material fracture toughness. Thus a complete conceptual scheme for fitness-for-service assessment using the J-integral was formulated.

The next step was to develop relationships of the J contour integral to applied strain and crack size. Curves displaying J as a function of ϵ for a given specimen configuration with a series of flaw sizes are

shown schematically in figure 2a. If the strain pattern remains uniform as crack size increases, the curves of figure 2a can be collapsed into a single curve for that specimen configuration (fig. 2b). Rules to develop an equivalent flaw size, \bar{a} , for a variety of configurations would lead to a single design curve. If, on the other hand, the form of the strain pattern were to change with flaw size, the individual J- ϵ curves would not collapse onto a unique design curve, and approximate methods for describing this behavior would be required for fitness-for-service assessments. To put the latter situation in perspective, recall that the LEFM analysis procedures are configuration dependent. This dependence is expressed mathematically by writing

$$K = \sigma \sqrt{\pi a} Y(a) \quad (1)$$

where K is the stress intensity factor, σ is the stress, and Y(a) is a geometry-dependent function. To provide experimental data for the J-vs.-strain curves described here schematically, the techniques referred to earlier were applied.

Previous techniques for measurement of J as a function of strain include the compliance technique and two techniques for direct measurement of the J-contour integral. The compliance technique [7] was tested in the work on the C-Mn ship steel described in Appendix A. This method was rejected because it was not considered appropriate for cracks 25% or less of the specimen width. A technique for direct measurement of the J-contour integral was developed and used for the linear elastic case by Kino and Herrmann [12], and a different technique applicable to rubber

was developed by Oh [11]. The method developed for the present study extended the experimental evaluation of Rice's path independent J-contour integral [6] to the elastic-plastic regime. According to Rice, the J-integral is given by

$$J = \int_{\Gamma} W dy - \vec{T} \cdot \frac{\partial \vec{u}}{\partial x} ds \quad (2)$$

where W is the strain-energy density, \vec{T} is the traction vector normal to the contour Γ surrounding the crack, x and y are Cartesian position coordinates, \vec{u} is the displacement vector, and ds is a length increment along Γ .

The strain-energy density is evaluated from strain gages mounted along a convenient path surrounding the crack tip using the relation

$$W = \int \sigma_{ij} d\epsilon_{ij} \quad (3)$$

where the σ - ϵ curve of an uncracked specimen serves as the function $\sigma_{22}(\epsilon_{22})$, and all the other components of the stress tensor are zero because the contour follows the free surface. The rotational contribution to J , $\vec{T} \cdot \frac{\partial \vec{u}}{\partial x}$ is evaluated by using displacement gages mounted along the x -direction component of the contour Γ . The nature of the strain energy and rotational contributions to J are shown in figure 3. Experimental details for measurements on single-edge-cracked specimens are given in Appendix B. The method of direct measurement of the J contour integral was found to be suitable for evaluating the applied J-integral as a function of strain for several different nonstandard specimen geometries with short cracks.

EXPERIMENTAL PROGRAM

Materials

Specimens of two different steels were tested. Preliminary experiments were conducted using C-Mn ship steel specimens. This steel was selected because of its extremely high toughness to prevent specimen tearing from interfering with measurements of the applied J-integral. This material had a yield strength of 340 MPa (49.3 ksi) and a tensile strength of 483 MPa (70.1 ksi). Its chemical composition is listed in table 1. HY130 steel is the principal specimen material of this program. The plate used had a yield strength of 933 MPa (135 ksi) and an ultimate tensile strength of 964 MPa (140 ksi). Its chemical composition and heat treatment are listed in table 1.

Table 1. Chemical compositions by weight percent and treatment for steels used in the experimental program.

C-Mn Ship Steel

Chemical composition, weight percent:

<u>C</u>	<u>M</u>	<u>P</u>	<u>S</u>	<u>Si</u>	<u>Cr</u>	<u>Ni</u>	<u>Mo</u>	<u>Cu</u>	<u>V</u>	<u>Al</u>
0.11	1.44	0.10	0.007	0.21	0.08	0.30	0.06	0.20	0.001	0.038
<u>Ce</u>	<u>Fe</u>									
0.0	bal									

Treatment: Silicon killed, vacuum degassed, aluminum added, normalized.

HY130 Steel

Chemical Composition, weight percent:

<u>Ni</u>	<u>Cr</u>	<u>Mo</u>	<u>V</u>	<u>C</u>	<u>Mn</u>	<u>P</u>	<u>Si</u>
5.00	0.42	0.53	0.043	0.11	0.76	0.005	0.03
<u>S</u> <td><u>Cu</u><td><u>Al</u><td><u>Co</u><td><u>Ti</u><td><u>Fe</u></td><td></td><td></td></td></td></td></td>	<u>Cu</u> <td><u>Al</u><td><u>Co</u><td><u>Ti</u><td><u>Fe</u></td><td></td><td></td></td></td></td>	<u>Al</u> <td><u>Co</u><td><u>Ti</u><td><u>Fe</u></td><td></td><td></td></td></td>	<u>Co</u> <td><u>Ti</u><td><u>Fe</u></td><td></td><td></td></td>	<u>Ti</u> <td><u>Fe</u></td> <td></td> <td></td>	<u>Fe</u>		
0.004	0.022	0.021	0.02	0.008	bal		

Treatment: Austenitized, quenched, tempered, quenched.

Technique

The experimental technique developed for the present study, direct measurement of the J-contour integral, is described in detail in Appendix B. This method uses strain gages and LVDT's to measure the quantities inside the J-integral directly; numerical integration is used to calculate the J-integral from these data.

Specimens

In this study, a total of 9 measurement runs have been completed to date. These include 4 single-edge-cracked specimens of C-Mn ship steel and 5 single-edge-cracked HY130 specimens. All specimens were approximately 9-cm wide and were pin loaded. Saw cuts were used to simulate cracks in most specimens. In others, fatigue cracks were used.

RESULTS

The results for the C-Mn steel specimens are discussed in Appendix A; the results for the HY130 single-edge-cracked specimens are interpreted briefly below.

Data accumulated on single-edge-cracked specimens (shown in fig. 4) indicate some important features of the dependence of J on applied strain and crack length. First, the functional form of the dependence of J on strain is usually parabolic, then linear. All credible theories and most of the experimental data support this behavior. The parabolic region at low strains is the region of linear-elastic-fracture-mechanics. Here the J-integral approach reduces to the well-known stress intensity factor approach. Second, the slopes of the linear parts of the J-vs.-strain curves depend on crack length. For fairly large cracks in

tension (as opposed to bending), the slopes are weakly dependent on crack length. As the crack length decreases to low values, the slope of the J-vs.-strain plot decreases sharply. In figure 4, the crack length at which this slope change occurs is less than 4 mm in a 90-mm wide specimen.

The interpretation of these results is believed to be as follows: for relatively large cracks, displacements imposed at the specimen ends are transmitted in full to the cracked cross section; they add to the strain field of the crack and produce a large applied J value. This behavior is described as net section yielding [13]. For relatively short cracks, like the 1-mm crack in figure 4, displacements imposed at the specimen ends are absorbed as plastic strain all along the specimen length; they add only slightly to the strain field of the crack and produce small applied J values. This behavior is described as gross section yielding [13]. It is important to note that cracks as small as 5% of the total cross section can exhibit net section yielding.

CONCLUSIONS

From the effort expended so far in this program the following conclusions have been reached:

1. Direct measurement of the J contour integral, supported by finite element analysis and theoretical modeling, is capable of providing accurate evaluation of the applied J-integral in the presence of short cracks (down to about 1 mm) in specimens simulating structural situations.

2. For relatively large cracks, displacements imposed at the specimen ends are transmitted in full to the cracked cross section; they add to the strain field of the crack and produce large applied J values (net section yielding). For relatively short cracks, displacements imposed at the specimen ends are absorbed as plastic strains all along the specimen length; they add only slightly to the strain field of the crack and produce small applied J values (gross section yielding). Cracks as small as 5% of the total specimen cross section have been found to exhibit net section yielding.

WORK IN PROGRESS

Work in progress includes testing and analysis for a series of different specimen geometries, including center, part-through, and double-edge-cracked base-metal specimens, center-cracked base-metal wide plates and welded specimens in small and large sizes. Finite element analytical studies are in progress at the University of Kansas to allow analytical replication of the experimentally observed behavior.

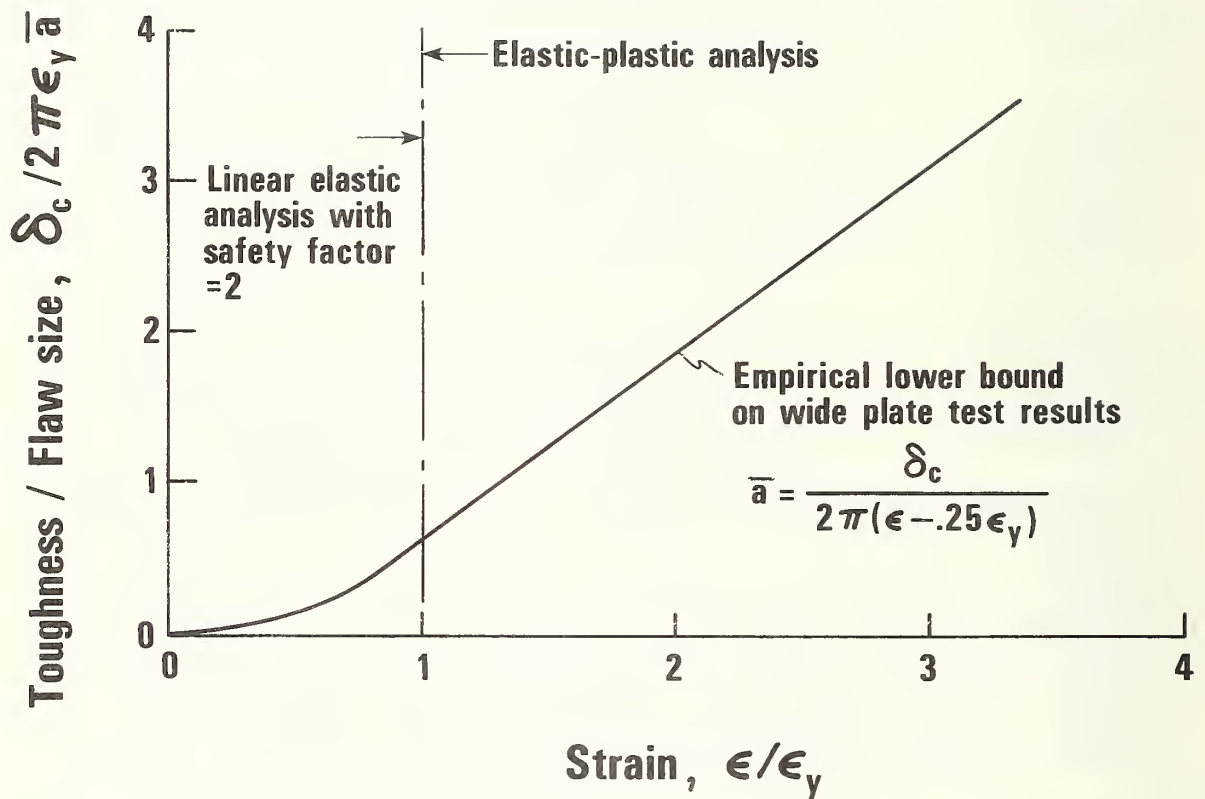
ADMINISTRATIVE INFORMATION

This report was prepared as part of the Fracture Control Technology Program under the sponsorship of Dr. H. H. Vanderveldt, Naval Sea Systems Command (SEA 05R15). The effort was monitored by Mr. John P. Gudas, David Taylor Naval Ship Research and Development Center, Code 2814, under Program Element 6276IN, Task Area SF 61-544-504.

References

- [1] Judy, R. W., Jr.; Crooker, T. W.; Corrads, J. A. ; Beach, J. E.; Hauser, J. A. Review of fracture control technology in the U.S. Navy. Presented at the Second Program Review, Fracture Control Technology for Ships and Submarines; 1979 November 30; Annapolis, MD.
- [2] McHenry, H. I.; Rolfe, S. T. Fracture control practices for metal structures. National Bureau of Standards (U.S.) NBSIR 79-1623; 1980 January. 114 p.
- [3] Brock, D. Fracture control approaches in Europe. Final report to the Naval Ship Research and Development Center; Battelle Columbus Laboratories, Columbus, OH; 1978 July 25. 45 p.
- [4] Anon.; Guidance on some methods for the derivation of acceptance levels for defects in fusion welded joints. British Standards Institution, London, England; 1980. 64-93.
- [5] Harrison, J. D.; Dawes, M. G.; Archer, G. L.; Kamath, M. S. The COD approach and its application to welded structures, in Elastic plastic fracture, ASTM STP 668. J. D. Landes, J. A. Begley, and G. A. Clarke, eds. Philadelphia, PA: American Society for Testing and Materials; 1973. 1-20.
- [6] Rice, J. R. A path independent integral and the approximate analysis of strain concentration by notches and cracks. J. Appl. Mech. 35: 379-386; 1968 June.
- [7] Begley, J. A.; Landes, J. D. The J integral as a fracture criterion, in Fracture toughness, ASTM STP 514. Philadelphia, PA: American Society for Testing and Materials; 1973. 1-20.

- [8] Landes, J. D.; Begley, J. A. The effect of specimen geometry on J_{IC} , in Fracture toughness, ASTM STP 514. Philadelphia, PA: American Society for Testing and Materials; 1972. 24-39.
- [9] Longsdon, W. A. Elastic plastic (J_{IC}) fracture toughness values; their experimental determination and comparison with conventional linear elastic (K_{IC}) fracture toughness values for five materials, in Mechanics of crack growth, ASTM STP 560. Philadelphia, PA: American Society for Testing and Materials; 1976. 43-60.
- [10] Bucci, R. J.; Paris, P. C.; Landes, J. D.; Rice, J. R. J integral estimation procedures, in Fracture toughness, ASTM STP 514. Philadelphia, PA; American Society for Testing and Materials; 1972. 40-69.
- [11] Oh, H. L. A simple method for measuring tearing energy of nickel rubber strips, in Mechanics of crack growth, ASTM STP 590. Philadelphia, PA: American Society for Testing and Materials; 1976. 104-114.
- [12] Herrmann, G.; Kino, G. S. Ultrasonic measurements of inhomogeneous stress fields. Proceedings of ARPA/AFML review of progress in quantitative NDE, AFML-TR-78-205. 1979 January. 447-451.
- [13] Turner, C. E., Methods for post-yield fracture safety assessment, in Post-yield fracture mechanics. D. G. H. Latzko, ed. London: Applied Science Publishers; 1979. 23-210.



Allowable flaw size, \bar{a} \Rightarrow fracture toughness, δ_c
 applied strain, ϵ
 material properties, $\epsilon_y = \frac{\sigma_y}{E}$

Figure 1. Crack-opening-displacement (COD) design curve.

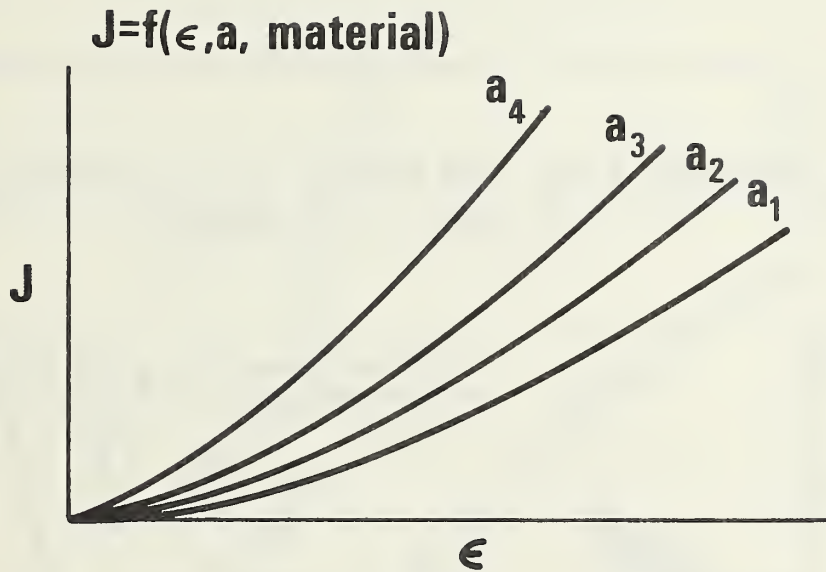


Figure 2a. Schematic plots of J-integral vs. strain.

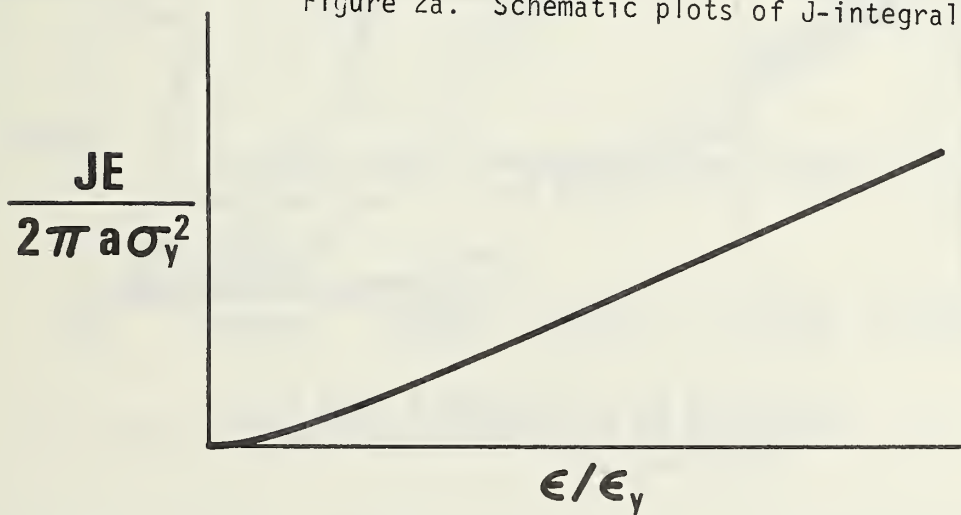


Figure 2b. Single curve formed from the curves of Fig. 2a by dividing ordinate, J , by crack length a , and a factor which includes material tensile properties.

DEFORMATION PATTERNS THAT CONTRIBUTE TO THE J-INTEGRAL

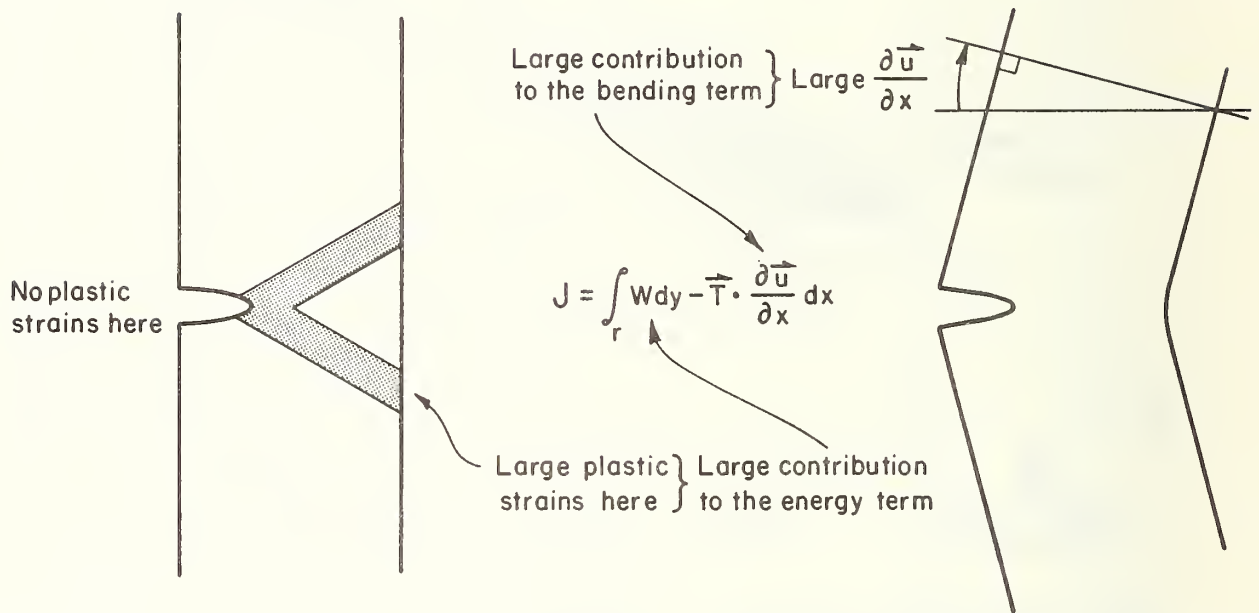


Figure 3. Sources of the strain energy and rotational contributions to J.

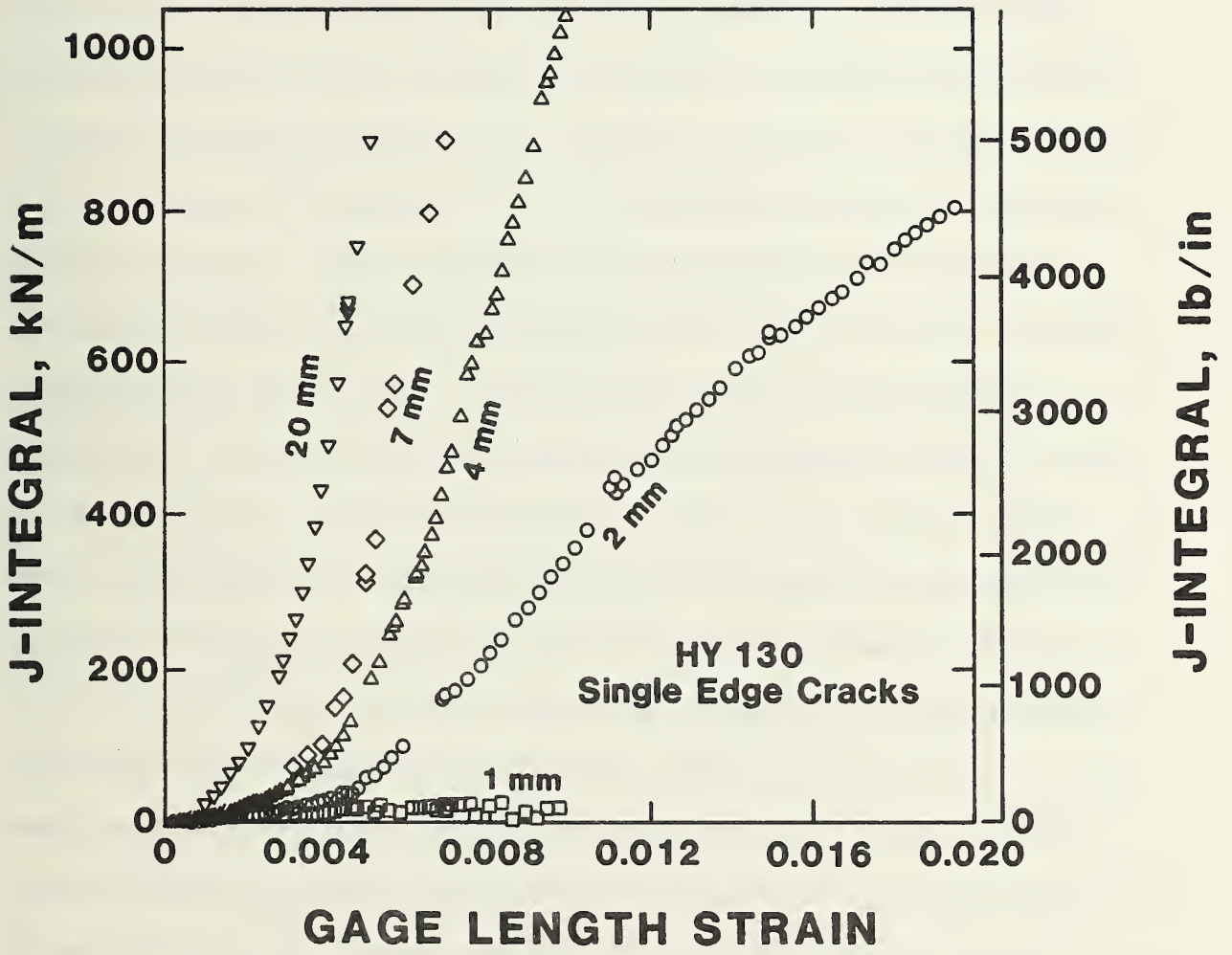


Figure 4 Measured J-integral plotted against strain for single-edge-cracked specimens. Crack lengths are noted on the graph.

APPENDIX A

EXPERIMENTAL METHOD FOR DIRECT EVALUATION OF THE J CONTOUR INTEGRAL

D. T. Read
Fracture and Deformation Division
National Bureau of Standards
Boulder, Colorado 80303

Key Words: Contour integral; direct evaluation; displacement; evaluation; experimental; J-integral, line integral; numerical integration; path independent; strain

ABSTRACT

A method for direct experimental evaluation of the J contour integral has been developed and used to measure J as a function of strain in tensile panels of high strength steel ($\sigma_y = 900$ MPa) under elastic-plastic loading conditions. The principle of the present method is to measure the integrand terms of J at suitable intervals along an appropriate contour and then to evaluate the integral. Because the resulting J values are based directly on the definition of J, no assumptions about the crack size or the stress-strain fields in the vicinity of the crack tip are necessary. This advantage is crucial in cases of very short cracks (less than 10% of the panel width), which are of special interest for structural applications. The integrand terms are measured with strain gages and linear variable displacement transducers (LVDTs) placed on an appropriate contour surrounding the crack. Load, LVDT-displacement, strain-gage, and crack-mouth-opening-displacement measurements are acquired, stored, and printed at each deformation increment, and the J-integral is evaluated numerically by a minicomputer. J-integral values are plotted against the average specimen strain in real time. Directly measured J-integral values and values calculated using linear elastic fracture mechanics agreed within 12% for average strain values between 10 and 90% of yield. The experimental uncertainties become significantly less for strains of several times yield than for strains below yield. This technique has been used to measure J as a function of strain in edge-cracked and center-cracked tensile panels with short cracks at strains beyond yield, cases for which closed-form solutions for J are not available.

INTRODUCTION

This paper describes a method for experimental evaluation of the J-integral as a function of stress or strain for single-edge cracks. The method is also applicable to through cracks and may be of interest for studies of surface cracks. The principle of the present method is to measure the integrand terms of J at suitable intervals along an appropriate contour and then evaluate the integral. Because the resulting J value is based directly on the definition of J, no assumptions about the crack size or the behavior of stress-strain fields produced by the action of the crack tip are necessary. This advantage is crucial in cases of very short cracks, which are of special interest for structural applications. The present method extends previous direct experimental evaluations of the J-integral in metals in the elastic range [1] and in rubber [2] to the case of metals in the plastic-strain range.

The J contour integral has been applied widely in characterizing the fracture toughness of metals [3-5] but its application to evaluation of the durability of structures containing cracks or similar defects has been delayed by the absence of information on the material J_{IC} value needed in a structural element containing a crack and subjected to a certain stress or strain. The present study, therefore, is complementary to current work advancing the use of the J-integral for materials characterization; it also extends current knowledge of applied J-integral values beyond the linear-elastic case where well-known and widely used handbook solutions [6] for the stress intensity K can be used to calculate the applied J-integral.

METHOD

The definition of the J-integral as given by Rice [7] is:

$$J = \int_{\Gamma} W dy - \vec{T} \cdot \frac{\partial \vec{u}}{\partial x} ds \quad , \quad (1)$$

where W is the strain energy density, \vec{T} is the traction vector, \vec{u} is the displacement vector, x and y are Cartesian position coordinates, and s is arc length along the contour. The contour chosen for direct measurement of the J-integral is indicated in Fig. 1a. Because of symmetry about the plane of the crack, only half of each specimen was instrumented. Tensile panels were selected because they have more accessible cracks, a larger possible range of crack-length-to-specimen-width ratios, and a greater relevance to structural situations than bend bars. The contour follows specimen free surfaces along the y -direction and traverses the tensile axis at a location away from the crack. Measurement of the J-integral along this contour requires determination of the strain energy density along the y -direction contour segments and measurement of traction and displacement vectors along the x -direction segments. The strain-energy density was obtained by using strain gages along the contour (Fig. 1b) and referring these strains to the stress-strain curve of an uncracked tensile specimen. The energy density of the uncracked specimen was calculated simply as the area under its stress-strain curve. Because the only nonzero stress component at the strain gages along the y -direction contour segments was the axial tensile stress, the strain-energy density value for a given strain was the same as that for the tensile specimen. The y -components of the traction and displacement vectors along the x -direction contour segments were measured using strain gages and LVDT's, respectively. Because the horizontal contour segment was chosen to be away from the crack, only the y -components of the traction and displacement were significant. Since the only significant stress at the contour was the y -direction

tensile stress, it could be obtained from the strain measured at the contour using the stress-strain curve of the uncracked tensile bar. The y-component of the traction was numerically equal to this stress. The y-direction displacement was measured at three locations along the x-direction contour segment. The change in displacement with position, du/dx , was calculated from the measured displacements. After determination of the terms of the integrand, the J-integral was calculated either (a) by numerical integration using predetermined values for the length of contour covered by each strain-energy density or traction-bending term or (b) by fitting the strain along each of the two y-direction contour segments with polynomials or selected nonlinear functions and then calculating strain-energy density values and performing the required integrations using the strains as given by the fitting functions. The method involving nonlinear fits to the measured strains was finally judged to be superior.

The specimen material used in the present study was HY-130 steel; the plate used had a yield strength of 933 MPa and a tensile strength of 964 MPa. Tensile panels with gage sections 30-cm long by 9-cm wide by 1-cm thick were used. Saw-cut notches were usually used instead of fatigue cracks to postpone tearing. Specimens having single-edge-notches with lengths of 1, 2, 4, 7, and 20 mm were tested. The specimens were instrumented as in Fig. 1b. Approximately eight strain gages were placed along each y-direction contour segment. Very small gages (active length of about 0.75 mm) were used near the mouth of short cracks. Three LVDT's were mounted along the x-direction contour. Strain gages were placed on the specimen between LVDT attachment locations. A clip-on gage was mounted in the crack mouth to measure crack-mouth-opening

displacement (CMOD). One 9- x 30-cm surface of each specimen was coated with brittle laquer to reveal strain patterns. The strain patterns produced were suitable for recording by photography.

A servohydraulic testing machine with a load capacity of 1 MN was used. The tests were run in displacement control. A commercially obtained analog-to-digital (A-D) conversion system with a 16-bit resolution was connected to the strain gages, LVDT's, testing-machine load cell, and CMOD gage. The A-D converter was connected to a commercially supplied minicomputer. The minicomputer system consisted of a processor, a dual floppy-disk data-storage unit, a digital plotter, and a printer.

The servohydraulic testing machine was controlled manually, but the data acquisition, on-line analysis, storage, printing, and plotting for each point of data were controlled by the minicomputer. For each deformation increment, each sensor was polled and its signal was converted from electrical to physical units and stored on floppy disk. Then the J-integral was calculated as described above. The J-integral, stress, CMOD, average strain (defined below), measured displacement values, and measured strain values were printed. Finally, each strain-gage output was plotted on a bar graph, and the calculated J-integral value was plotted against average strain. The average strain for this purpose was taken as the average of the three LVDT displacements divided by the specimen gage length. These displacements included contributions from the strain field of the crack as well as contributions from the strain that would have existed in the absence of the crack.

In the course of a typical test, first the instrumented specimen was mounted in the testing machine, and all of the instrumentation was connected and checked for proper function. When all the apparatus was performing properly, a zero-load data point was taken, and the specimen was extended by a preselected amount. Then the computer was allowed to proceed through the data acquisition-storage-calculation-print-plot procedure described above. The specimen was then extended further and the procedures repeated. The strain patterns revealed by the brittle laquer coating were photographed periodically throughout the test. Tests were terminated for two reasons: specimen tearing or gage failure. Tearing occurred before strain-gage failure in almost all cases.

About a hundred data points, each consisting of about twenty-five measured strain, displacement, and load values, were obtained during a typical test. The maximum average strain (defined above) attained during a test ranged from around 1.5 times yield for relatively deep notches to near 9 for shallow notches.

The stored data were used for posttest reanalysis, corrections, and replotting. A large-scale computer was used for the nonlinear fits and for detailed plotting of the strain and displacement data.

RESULTS AND DISCUSSION

The J-vs.-strain data for the tests described here are shown in Fig. 2. These curves consist of an elastic part at low strains and a plastic part at high strains. In the elastic region, the J-vs.-strain

curve is parabolic, and in the plastic part the curve is linear for most specimens, both as expected from previous studies [8,9].

The present technique of direct evaluation of the J contour integral requires subtraction of the energy density integral along the notched side (AB in Fig. 1b) from that along the unnotched side (CD in Fig. 1b) to obtain the energy density term, $\int_{\Gamma} W dy$, and subtraction of the displacement measured between points A and F from that between C and E to obtain the traction-bending term, $\int T_y \cdot (du_y/dx) \cdot ds$. (The result for the traction-bending term is insensitive to the displacement measured between points G and H because it is essentially cancelled out in the integration procedure.) The shorter the crack, the more nearly equal will be the two terms of each of these subtractions; it is the equality of the terms in each subtraction that causes J to be zero when the crack length is zero. The experimental uncertainty in the differences between the two nearly equal energy density integrals and the nearly equal displacements is much larger than the experimental uncertainty in either individual energy-density integral or displacement. This is shown in Table 1, which lists experimental uncertainties in energy density integrals, displacements, and the J-integral for the specimen with the 4-mm crack. The uncertainties in individual measured quantities were estimated from differences among measured values and differences between measured and expected values. Uncertainties in the energy density and J-integrals were estimated from the uncertainties in the individual measured quantities by using standard procedures from the theory of propagation of errors. Table 1 also shows that the uncertainty in J in the plastic-strain range is noticeably smaller than that in the elastic-strain range.

Table 1. Propagation of experimental uncertainties in direct measurement of the J contour integral. Data for HY-130, single edge notch, $a = 4$ mm.

Uncertainty	Elastic part	Plastic part
In larger integrated energy density term	1%	1%
In J from energy density terms alone	7.6%	2%
In LVDT displacement	1%	1%
In J from LVDT displacement alone	9.5%	2%
In J (combined uncertainty)	12 %	3%

The energy density integrations were performed numerically directly on the experimental data, on polynomials fitted to the data, and on nonlinear functions fitted to the data. The method involving nonlinear fits was judged to be the best. Figure 3 shows the measured strains as a function of position along the contour segment DC for the 4-mm crack-length specimen for a point of data in the plastic-strain range. Shown for comparison are three functional forms for the strain used in the energy density integral. Although the nonlinear function consisting of a Gaussian peak plus a three-term polynomial appears to give the best fit, the peak of the fitted function is well above the maximum measured strain. Examination of the specimen strain pattern as revealed by the brittle laquer coating showed that the highest strains occurred at the strain gage at $x = 5.4$ cm, and therefore, that the fitting function was in error. By adding a fictitious strain value linearly interpolated halfway between the values at 5.4 and 7.9 cm from the plane of the

crack, the fitted curve was brought down to the locus shown as a dashed line. From this exercise it was concluded that the uncertainty in the J-integral from improper fitting could be about $\pm 8\%$, but that careful analysis could bring this down.

Lower uncertainties could also be obtained by using more strain gages along contours, such as DC, or by using the correct functions for strain vs. position along contour segments AB and CD to fit the measured strain values. Unfortunately, the correct functional form for the specimens of this study is unknown.

The comparison between the measured results and the linear-elastic handbook formula for K was made by converting the measured J-integral values to stress intensity (K) values through the equation

$$K = (JE)^{1/2} \quad (2)$$

where E is Young's modulus, and plotting K against nominal applied stress. An example is shown in Fig. 4. In this figure a linear relationship between experimentally measured K values and stress, with some experimental scatter superposed, is seen for the low- and medium-stress regions. At high stresses, K increases rapidly with stress because of the formation of a plastic zone of significant size at the crack tip. In linear elastic fracture mechanics, K is related to stress by equations of the form

$$K = \sigma \cdot f \quad (3)$$

where σ is the applied stress and f is a function of crack length and specimen width. Experimental values of the coefficient f were obtained by manually fitting the linear parts of the experimental K- σ data sets

to straight lines. The slopes of the lines were taken as the experimental f values. By comparing the experimental and theoretical f values, the agreement between measured and theoretical J-integral values can be assessed. In Table 2, reasonable agreement between measured and theoretical values of f can be seen.

The results obtained with both the nonlinear fit procedure and the no-fit procedure were close to the expected values. The polynomial fitting procedure was rejected because the fitted strains were not consistently close to the measured strains. The nonlinear fit procedure was adopted for final data analysis because it was considered to be less subjective than the no-fit procedure. For the numerical integration of strain-energy values in the no-fit procedure, the contour segments AB and CD were divided into intervals such that each interval contained one strain gage. A consistent procedure for selecting the boundaries between intervals was followed, but this procedure was selected in an essentially arbitrary manner and was considered subjective. An element of subjectivity was also present in the selection of the fitting functions used in the nonlinear fit method, but since these functions provided consistently good fits to the data, the results were considered to be approximately equivalent to the results that would have been obtained if the correct functional form were known.

No plasticity corrections were used in the comparisons of Table 2. The appropriateness of using only the linear-elastic terms is seen from the linear dependence of K on σ in the region of the comparison and is confirmed by the linear relation between CMOD and stress in the region

Table 2. Calculated and measured values of $f = dK/d\sigma$ for single-edge-notched HY-130 tensile panels.

Crack Length (mm)	Calculated f ($m^{1/2}$)	Measured f (no fit) ($m^{1/2}$)	Measured f (polynomial fit) ($m^{1/2}$)	Measured f (nonlinear fit) ($m^{1/2}$)
2	0.0898	0.0999	0.0728	0.089
4	0.1287	0.1366	0.1242	0.140
7	0.1747	0.1668	0.1493	0.163
20	0.3587	0.3567	0.3444	0.355

of the comparison (Fig. 5). Plasticity effects on the effective crack length show up in Fig. 5 only at stresses above 720 MPa for the specimen with the 4-mm notch.

It is concluded that good agreement has been obtained between J-integral values predicted from linear-elastic-fracture mechanics and values obtained experimentally by direct evaluation of the J contour integral. The agreement obtained in the linear-elastic region indicates that the uncertainty in the J-integral values obtained in the plastic region, which are the real focus of the present study, may be expected to be about 5% or less.

Another estimate of the experimental uncertainty was made by comparing values in the plastic strain region calculated by the no-fit and non-linear-fit methods. Differences of up to 10% were obtained. Accordingly, an uncertainty of $\pm 10\%$ was ascribed to the data produced by the present method for direct evaluation of the J contour integral. Larger errors can occur if the measured displacements include erroneous contributions from, for example, bending of the specimen. The measured displacements for the 2-mm-crack case listed in Table 2 required a correction for bending. Such bending might occur if the specimen were not

machined to adequate straightness or if the pin holes were not centered. These errors can be detected by comparison of measured displacements with expected results obtained from experience or analysis.

The present results are now compared with the previously developed extended-perfect-plasticity theory [10]. The J-integral-vs.-strain curves for each specimen can be divided into elastic and plastic regions. For the elastic region, linear elastic fracture mechanics (lefm) provides an appropriate theoretical description of the experimental situation. The experimental data were shown earlier to be in agreement with lefm predictions for the elastic region. The extended-perfect-plasticity theory is now applied to the plastic-strain range. First, the total J-integral is regarded as the sum of an elastic and a plastic part:

$$J = J_e + J_p \quad (4)$$

The linear dependence of J_p on gage-length strain is expressed as

$$J_p = M \cdot \sigma_f \cdot v_p \quad (5)$$

where σ_f is the material flow stress and v_p is the plastic part of the displacement applied at the specimen ends.

Differentiating we obtain

$$(dJ/dv) \cdot (1/\sigma_f) = M. \quad (6)$$

A straight line was determined by eye through each data set for J vs. strain in the plastic region, and experimental M values were calculated from the slopes of these lines and Eq. 6; these values are plotted in Fig. 6. Also shown in Fig. 6 is a dashed line calculated by the extended-

perfect-plasticity theory:

$$M = 1 - f' + \frac{[2f + (1-2\alpha)(1-f')]}{\sqrt{1 + 2f(1-2\alpha) - 2\alpha(1-\alpha)}}$$

where a = crack length, $\alpha = a/W$, W = specimen width, $f' = \partial f / \partial \alpha$, $f = \alpha_0 (1 - e^{-\alpha/\alpha_0})$, $\alpha_0 = a_0/W$, and a_0 = an adjustable parameter. The value of the parameter a_0 used in the calculations was chosen as 11 mm to optimize the fit of the theory to the data. The utility of this extended-perfect-plasticity model is that it provides a method for interpolating between large crack sizes, where theories of the type discussed by Rice, Paris, and Merkle [11] are expected to describe experimental results and very short crack sizes, where J must approach 0 as crack length approaches 0. The author believes that this region of short crack sizes will prove important in yielding fracture mechanics.

CONCLUSION

Direct experimental measurements of the J contour integral have been accomplished in a high-strength steel in the elastic-and plastic-strain ranges.

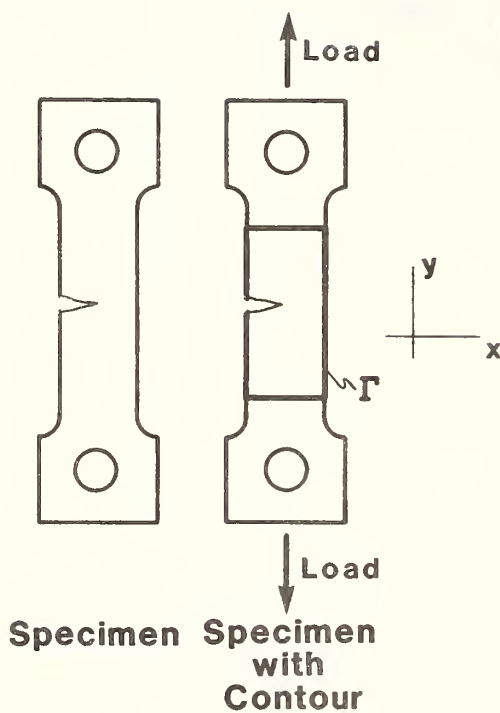
ACKNOWLEDGMENT

Helpful discussions with H. I. McHenry, technical assistance by J. D. McColskey, and the financial support of the United States David Taylor Naval Ship Research and Development Center, Annapolis, MD through J. P. Gudas, Project Monitor, are appreciated.

REFERENCES

1. H. L. Oh, "A Simple Method for Measuring Tearing Energy of Nickel Rubber Strips," Mechanics of Crack Growth, ASTM STP 590, American Society for Testing and Materials, Philadelphia, 1976, pp. 104-114.
2. G. Herrmann and G. S. Kino, "Ultrasonic Measurements of Inhomogeneous Stress Fields," Proceedings of ARPA/AFML Review of Progress in Quantitative NDE, AFML-TR-78-205, Air Force Materials Laboratory, 1979, pp. 447-451.
3. W. A. Logsdon, "Elastic Plastic (J_{IC}) Fracture Toughness Values: Their Experimental Determination and Comparison with Conventional Linear Elastic (K_{IC}) Fracture Toughness Values for Five Materials," Mechanics of Crack Growth, ASTM STP 560, American Society for Testing and Materials, Philadelphia, 1976, pp. 43-60.
4. J. A. Begley and J. D. Landes, "The J Integral as a Fracture Criterion," Fracture Toughness, ASTM STP 514, American Society for Testing and Materials, Philadelphia, 1972, pp. 1-20.
5. J. D. Landes and J. A. Begley, "The Effect of Specimen Geometry on J_{IC} ," Fracture Toughness, ASTM STP 514, American Society for Testing and Materials, Philadelphia, 1972, pp. 24-39.
6. H. Tada, P. Paris, and G. Irwin, The Stress Analysis of Cracks Handbook, Del Research Corporation, Hellertown, Pennsylvania, 1973.
7. J. R. Rice, "A Path Independent Integral and the Approximate Analysis of Strain Concentration by Notches and Cracks," Journal of Applied Mechanics 35, 1968, pp. 379-386.
8. R. J. Bucci, P. C. Paris, J. D. Landes, and J. R. Rice, "J Integral Estimation Procedures," Fracture Toughness, ASTM STP 514, American Society for Testing and Materials, Philadelphia, 1972, pp. 40-69.

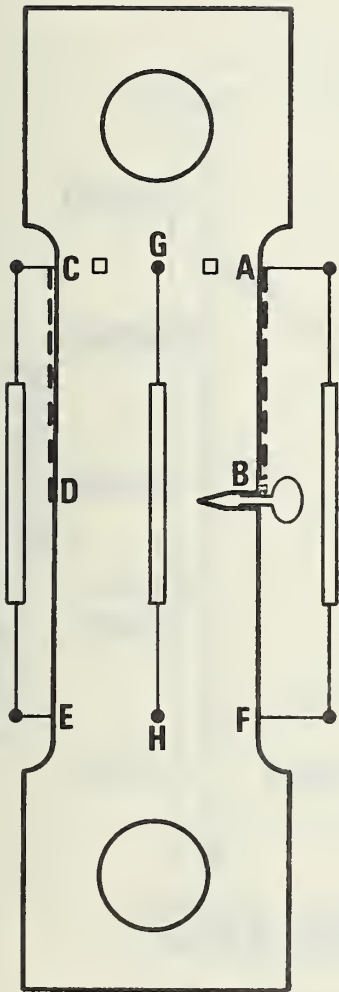
9. J. A. Begley, J. D. Landes, and W. K. Wilson, "An Estimation Model for the J-Integral," Fracture Analysis, ASTM STP 560, American Society for Testing and Materials, Philadelphia, 1974, pp. 155-169.
10. D. T. Read and H. I. McHenry, "Strain Dependence of the J-Contour Integral in Tensile Panels," Proceedings of the Fifth International Conference on Fracture, 1981, to be published.
11. J. R. Rice, P. C. Pris, and J. G. Merkle, "Some Further Results of J-Integral Analysis and Estimates," Progress in Flaw Growth and Fracture Toughness Testing, ASTM STP 536, American Society for Testing and Materials, Philadelphia, 1973, pp. 231-245.



$$J = \int_{\Gamma} W dy - \vec{T} \cdot \frac{\partial \vec{u}}{\partial x} ds$$

- x, y Position coordinates
- W Strain energy density
- \vec{T} Traction vector
- $\frac{\partial}{\partial x}$ Partial derivative with respect to x
- \vec{u} Displacement vector

Figure 1 (a). Contour chosen for direct evaluation of the J contour integral for single-edge-cracked specimens.



- ⋮ Small strain gages
- Strain gages
- ⏏ LVDT's
- ⊖ CMOD gage

**Specimen with
Instrumentation**

Figure 1 (b) Instrumentation placement for direct evaluation of the J contour integral for single-edge-cracked specimens.

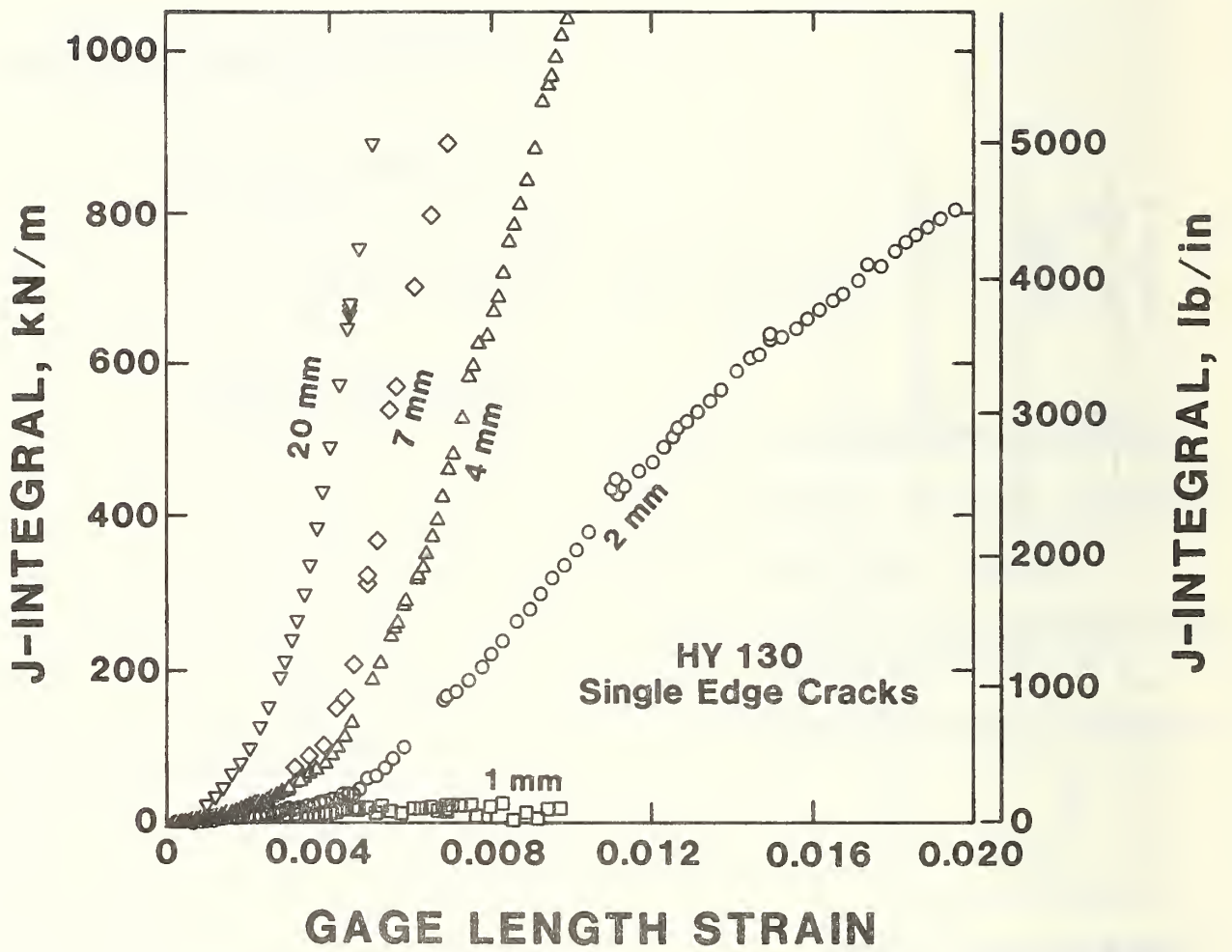


Figure 2. Measured J-integral plotted against strain for single-edge cracked specimens. Crack lengths are noted on the graph.

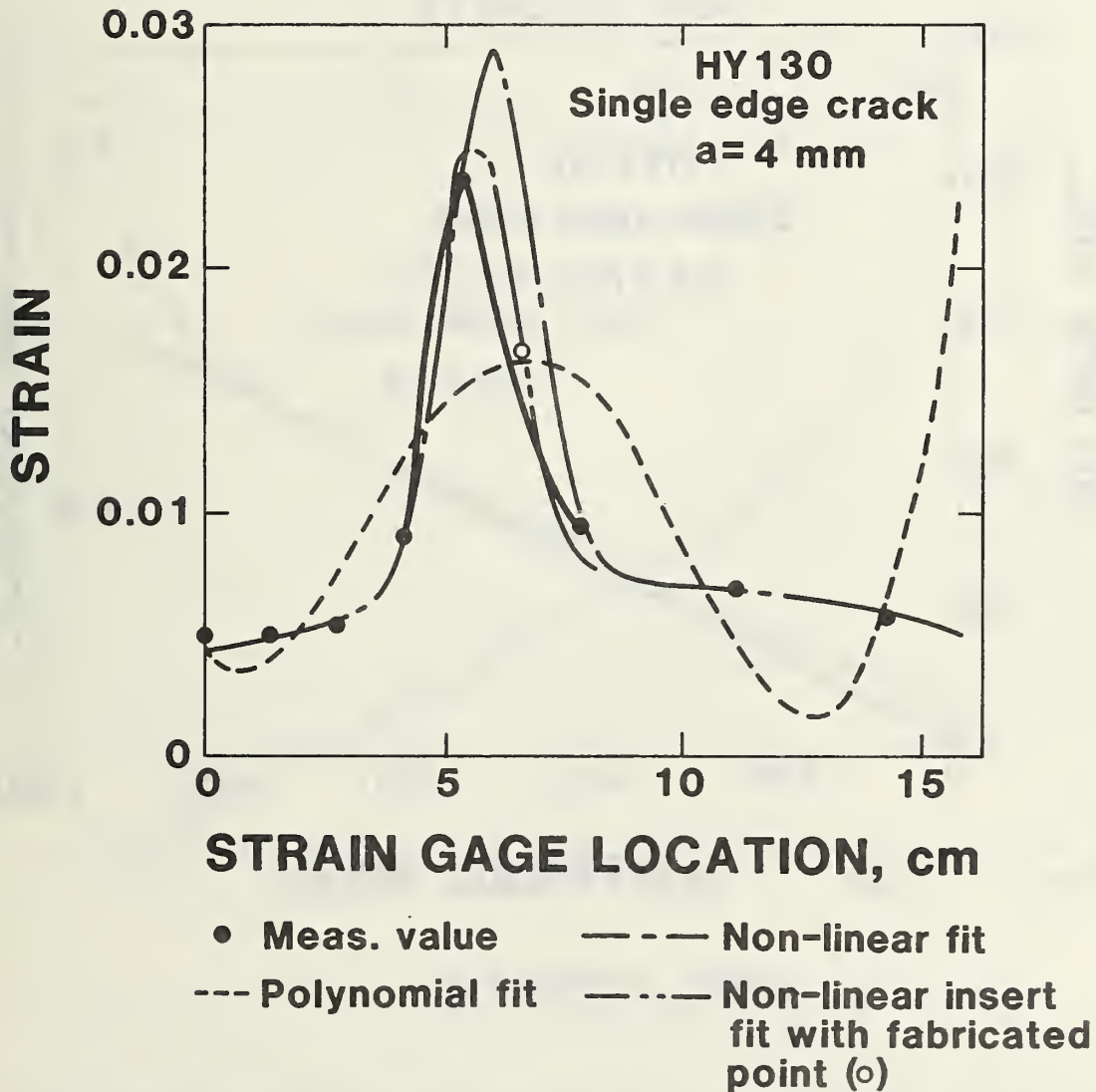


Figure 3. Strain as a function of location along contour segment AB (Fig. 1b). The zero of location is the crack plane. Included are measured values, showing position increment used for direct integration, polynomial fit, nonlinear fit, and nonlinear fit to real data plus one fictitious data point.

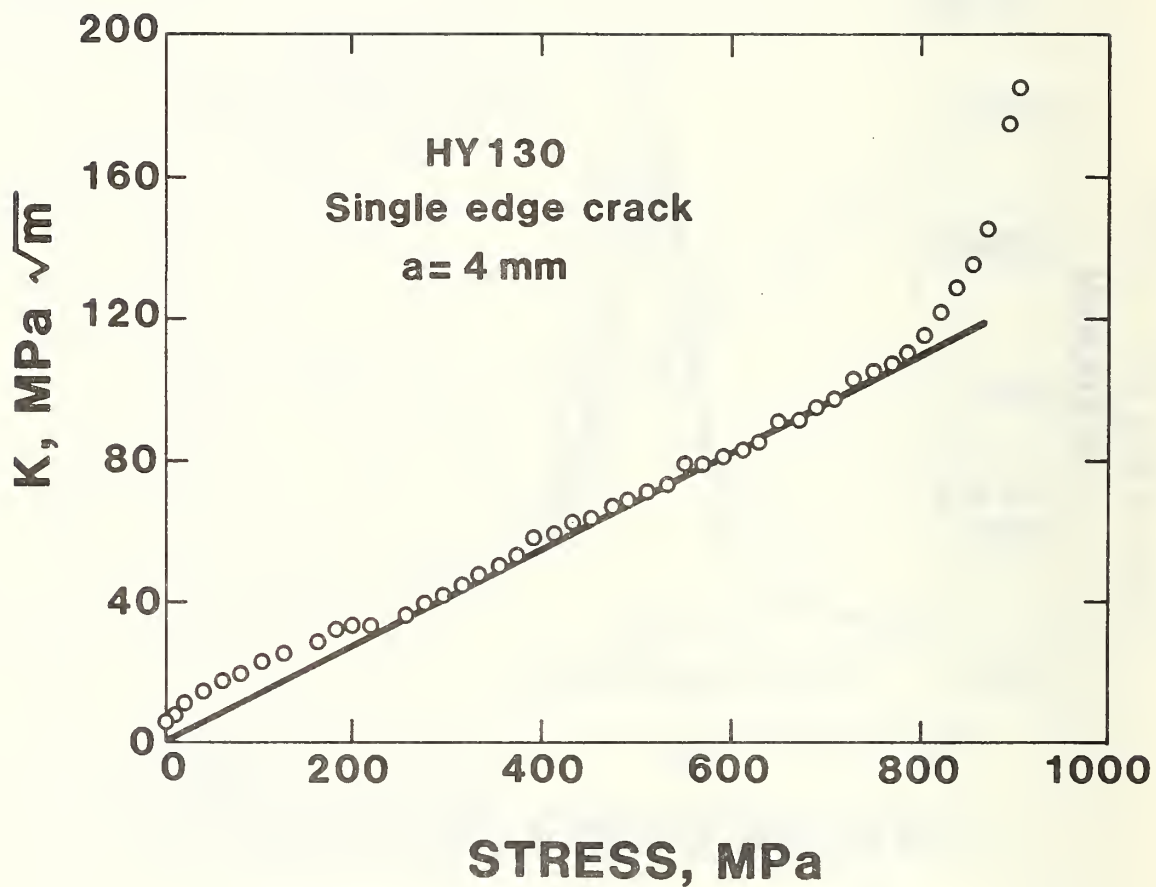


Figure 4. Stress intensity, K, plotted against nominal applied stress for the specimen with the 4-mm crack.

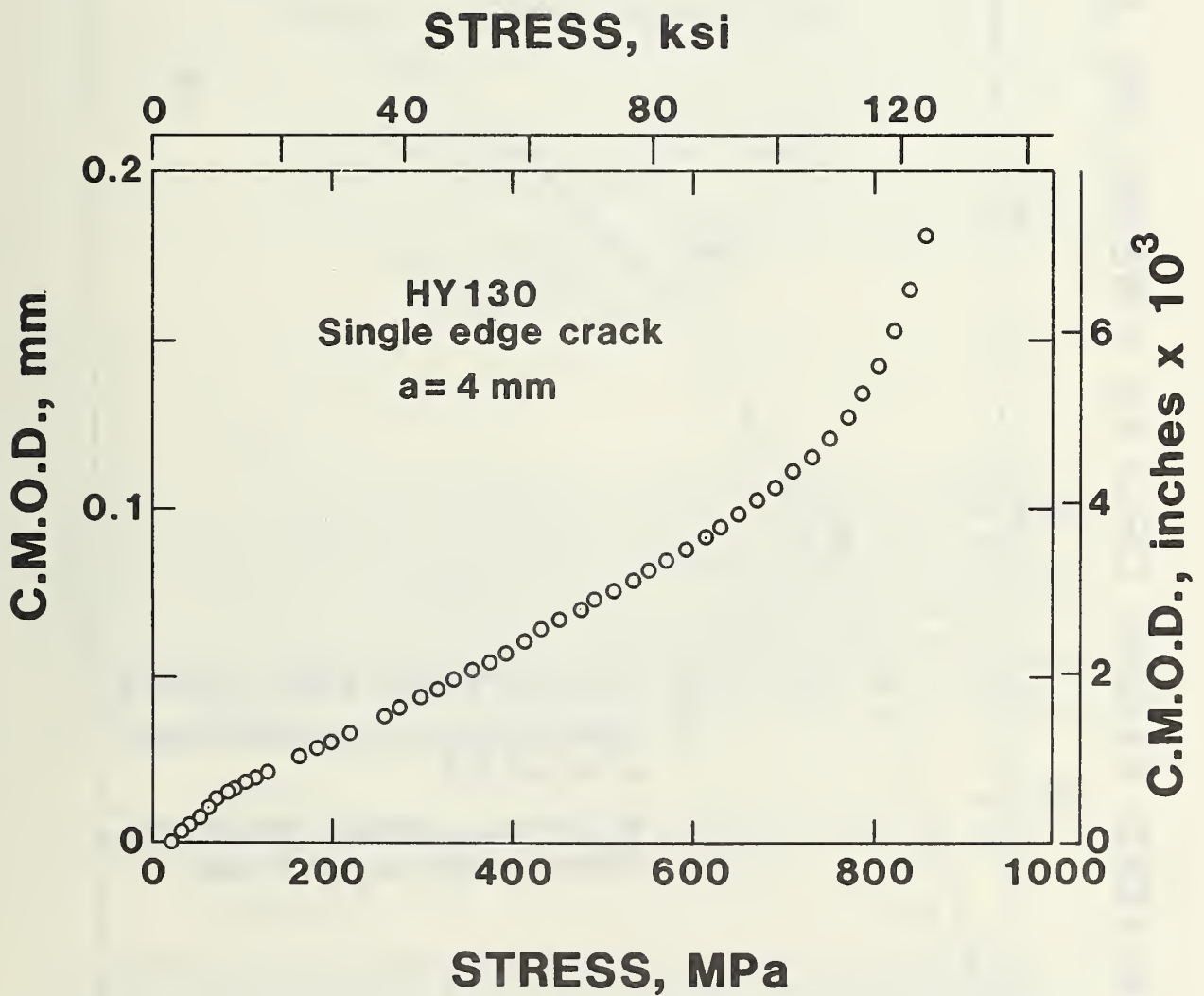
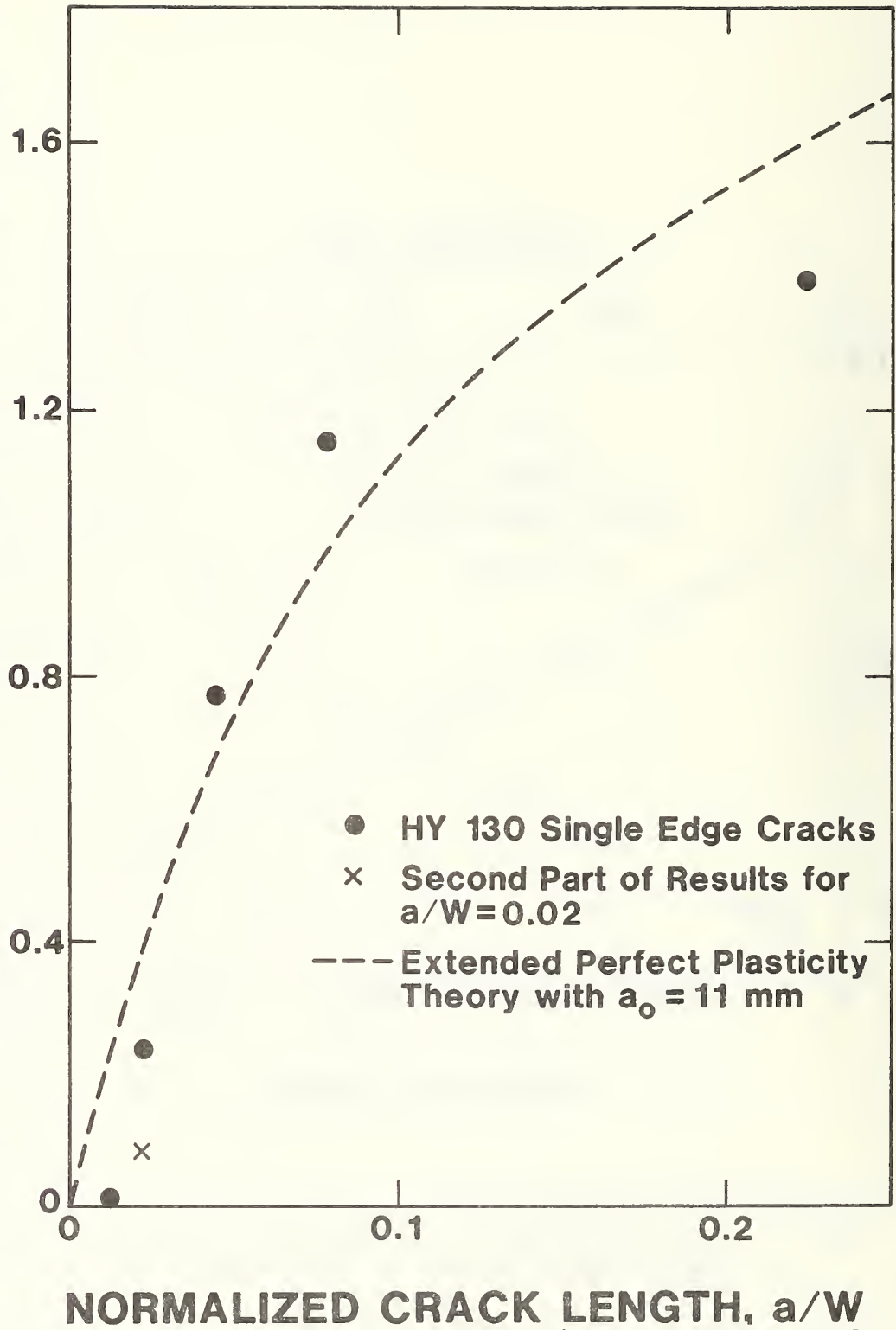


Figure 5. Crack-mouth-opening-displacement (CMOD) plotted against nominal applied stress for the specimen with the 4-mm crack.

NORMALIZED SLOPE OF J vs V RESULTS, $\Delta J/\sigma_y \Delta v$



NORMALIZED CRACK LENGTH, a/W

Figure 6. Measured values of $M = (1/\sigma) dJ/dV$ for four single-edge-cracked specimens plotted against crack length. The curve through the data was determined by eye. The dashed line is an approximate theoretical result.

APPENDIX B

Reprinted from

ADVANCES IN FRACTURE RESEARCH

Edited by

D. FRANCOIS *et al*

PERGAMON PRESS OXFORD and NEW YORK 1980

STRAIN DEPENDENCE OF THE J-CONTOUR INTEGRAL IN TENSILE PANELS*

D. T. Read and H. I. McHenry
Fracture and Deformation Division
National Bureau of Standards
Boulder, Colorado 80303

ABSTRACT

The J contour integral has been experimentally measured as a function of applied strain for single edge notch tensile panels under elastic-plastic loading conditions. The results have been compared to analytical predictions based on finite element analysis and to theoretical estimates based on models representing the two behavioral extremes, uniform strain and perfect plasticity. The experimental, analytical and theoretical results have the expected form: the J-integral initially increases as the square of the applied strain, and at strains above yield the J-integral is a linear function of strain. The experimental and analytical results are in reasonable agreement, while the uniform strain and perfect plasticity models under- and over-estimate J respectively. An extension of the perfect plasticity model is proposed to treat behavior between these two limiting cases.

KEYWORDS

Crack driving force; elastic-plastic conditions; J-integral; fracture mechanics; tensile panels; finite-element-analysis; theoretical models

INTRODUCTION

The J-integral has gained widespread acceptance as a measure of the driving force for fracture under elastic-plastic conditions, that is, when notch tip plasticity is extensive. This report describes experimental measurements of applied J-integral values as a function of strain in simple configurations relevant to structural components. The experimental results are compared with results obtained from finite element analysis and theoretical models.

EXPERIMENTAL PROGRAM

Experimental measurements of the applied J value as a function of strain for several notch lengths have been performed. Three different experimental approaches were applied to allow verification of results: direct measurement of the contour integral; measurement of the pseudo-potential-energy change with crack extension (compliance technique); and measurement of crack tip opening displacement (CTOD). Each approach applies a known relationship between J and some set of experimentally measurable quantities, as described in detail by Read and McHenry (1980).

Experimental Procedures

The material chosen for the present study was a normalized C-Mn steel with a yield strength of 340 MPa. Single-edge-notched tensile panels with gage section 100 mm wide, 348 mm long, and 12 mm thick were tested with notch lengths of 0, 2, 10, 30 and 46 mm. Tension-tension fatigue precracking was used to sharpen the crack tips (except for the 2 mm notch which was tested with the notch tip as cut with a jeweler's saw).

The instrumentation required for direct measurement of the J contour integral consisted of twenty electrical resistance strain gages and three linear variable displacement transducers (LVDT's) mounted on the specimen (Fig. 1) and a minicomputer for acquisition and storage of the strain and displacement values. The terms of the integrand were derived from the measured strain and displacement data and the integration was performed numerically using the trapezoidal rule.

A qualitative measure of the shape of the strain fields around the crack tips was obtained by coating the specimen gage sections with brittle lacquer before straining and then observing darkened regions in the lacquer which corresponded to regions of high specimen strain. Photographs were made of the strain patterns at regular intervals during the test.

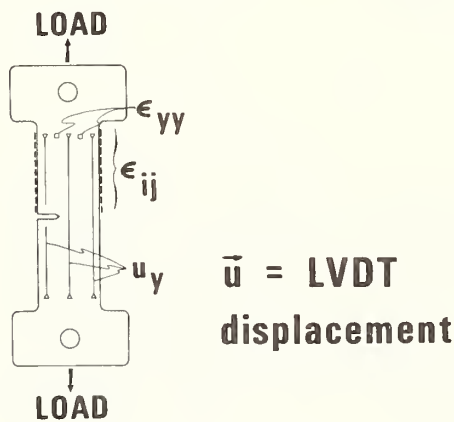


Fig. 1. Experimental arrangement for direct measurement of the J-contour-integral.

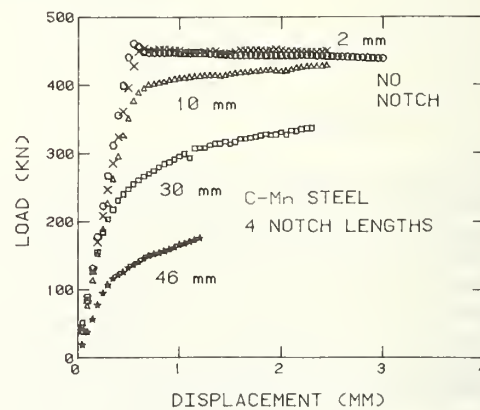


Fig. 2. Load plotted against displacement for all specimens.

RESULTS

The load-displacement records are shown in Fig. 2. J-integral values were determined as a function of strain for the four notched tests. Strain was defined as the average displacement measured by the three LVDT's over a gage length of 348 mm. Data points were obtained at strain intervals of about 0.00015. J-values were determined by the direct evaluation of the J-contour-integral, Fig. 3, and by the compliance method, Fig. 4. The CTOD at maximum strain was measured using the replication technique; the results are shown in Table 1. The general form of the J vs. ϵ curves is a parabolic dependence of J on strain at low strains and a linear dependence at strains above yield. The parabolic-then-linear form of the J- ϵ curves consistent with previous experimental studies employing the compliance technique by Bucci, Paris,

Landes and Rice (1972), with theoretical studies by Begley, Landes and Wilson (1974), and with theoretical and experimental studies in support of British COD design curve (Burdekin and Stone, 1966). Significant deviations from the parabolic-then-linear dependence of the J on strain were observed in certain of the tests of the present study. In the 2 mm notch, the rapid rise in J at the yield strain occurred as narrow shear bands emanated from the crack tip, Fig. 5. At higher strains (>0.0025), the shear bands spread due to strain hardening, and effectively masked the 2 mm notch so that J no longer increased with strain. In the 10 mm notch test, the shape of the J- ϵ curve was influenced by plastic deformation near the holes machined through the specimen to attach the LVDT's. Note that these holes did not cause plastic deformation (detectable by cracking of the brittle lacquer) in the deeper-notch tests; holes were not used in the 2 mm notch specimen. The results for the 46 mm notch test were influenced by the loading history which included complete unloadings at strain values of 0.0012 and 0.0019. In addition, shear strains, which are greater for the deeply notched case, were not accounted for in the direct measurement of J.

Table 1 Crack tip opening displacements (CTOD) and resulting J values, calculated using $m = 2.2$.

Notch length (mm)	Strain	CTOD (mm)	J(kN/m)
10	0.011	1.57	1152
30	0.0077	1.90	1394
46	0.0034	0.56	409

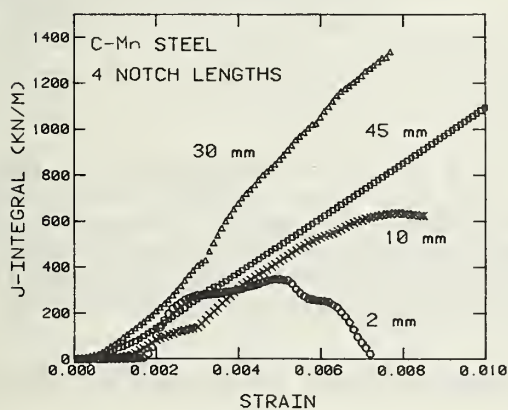


Fig. 3. Experimental results for the J-integral obtained by direct measurement of the contour integral.

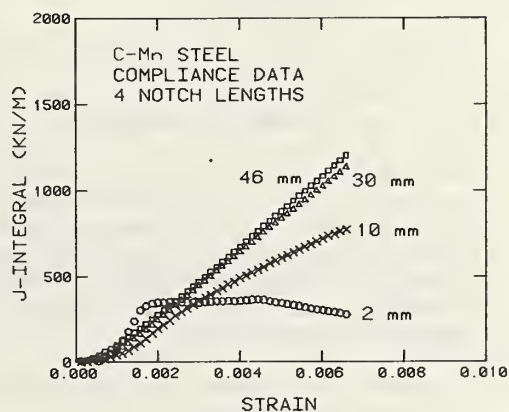


Fig. 4. Experimental results for the J-integral determined by the compliance technique.

Analytical Results

The two-dimensional elastic-plastic finite element analysis computer code of Gifford (1975, 1978) and Hilton and Gifford (1979) was used to calculate J-integral vs. strain. This program incorporated special nonlinear crack tip elements and conventional 12-node quadrilateral isoparametric elements. Finite element analysis calculations of J vs strain were carried out for 30 and 46 mm single-edge-notches to model the experimental situation. Limitations of the finite element analysis program in the treatment of large strains prevented calculation of results for the 2 mm

notch and prematurely terminated the results for the 10 mm notch. The general form of the finite element results, shown in Fig. 6, was parabolic-then-linear as expected.



Fig. 5. Photograph of strain pattern revealed by brittle lacquer, in C-Mn steel specimen with 2.25 mm notch.

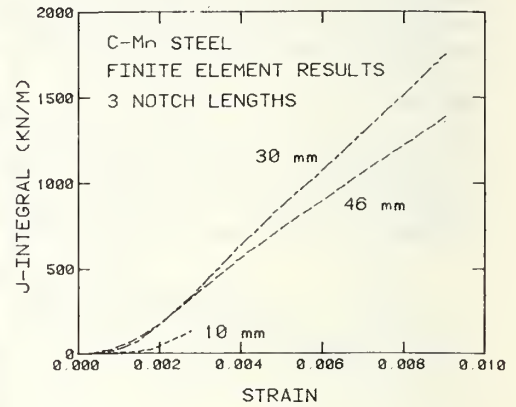


Fig. 6. Finite element results simulating the behavior of two specimens of the present study in the 46 mm notch and the 30 mm notch, and partial results for the 10 mm notch.

THEORETICAL MODELING

Three simple theoretical models giving J as a function of strain were considered in the present study. The case of a small notch in a large, uniformly strained panel was treated by Begley, Landes, and Wilson (1974); their result is referred to as the uniform strain model. The case of perfect plasticity was treated by Rice, Paris, and Merkle (1973). The perfect plasticity model was extended for the present study by adding a term to explicitly account for the stress-strain singularity at the crack tip in a simple manner.

The uniform strain model as developed by Begley, Landes, and Wilson (1974) resulted in the following expression for J :

$$J = \frac{\sigma_y^2}{E} \pi a \left(\frac{\epsilon}{\epsilon_y}\right)^2 \quad \text{for } \epsilon/\epsilon_y \leq 1 \quad (1a)$$

$$J = \frac{\sigma_y^2}{E} \pi a (2\epsilon/\epsilon_y - 1) \quad \text{for } \epsilon/\epsilon_y \geq 1 \quad (1b)$$

These formulas were derived for the case of a notch that is small enough that plastic strains are distributed throughout the panel rather than concentrated at the notch section. This situation minimizes J , and therefore, the uniform strain model is a lower bound solution for J vs. ϵ .

The elastic-perfectly plastic model for J as a function of strain follows the work of Paris, Tada, Zahoor, and Ernst (1979). Limit load per crack tip, P , is governed by yielding of the ligaments ($W - a$):

$$P = \sigma_y (W - a) T \quad (2)$$

and plastic displacements, Q_p , are concentrated at the crack tips, that is,

$$J_p = Q_p \sigma_y \quad (3)$$

where J_p is the plastic component of J . Adding the elastic component, J_e , yields:

$$J = J_e + J_p = \sigma^2 \pi a / E + Q_p \sigma_y \quad (4)$$

The strain distribution assumed in this model maximizes J , and therefore the perfect plasticity model usually provides an upper bound solution for J vs. ϵ .

Equation 2 neglects the existence of a stress-strain singularity at the crack tip. A simple way to approximately include the singularity is to postulate a line tensile force which operates along the crack tip perpendicular to the crack plane. This force was assumed to be proportional to a for $a/W \leq 0.1$ and to approach a constant value for longer cracks. A convenient functional form for such a force is the exponential relationship:

$$F = F_0 (1 - e^{-a/a_0}). \quad (5)$$

Here, F is the force across the crack tip per unit thickness and F_0 and a_0 need to be chosen. A relationship between F_0 and a_0 was derived by requiring J to approach zero as a approaches zero. After application of this relationship only one adjustable parameter, a_0 , is needed to fix F .

This force is regarded as a simplification of the Hutchinson (1968), Rice and Rosengren (1968) (HRR) Stress-strain field. In the extended perfect plasticity model, the spatial dependency of the HRR strainfield is ignored; the force, F , is considered to be concentrated at the crack tip. The strain independence of this force is consistent with the low strain hardening of the C-Mn steel used in the experimental program.

Using the crack tip force, the load required to extend a notched specimen at displacements above the yield displacement is calculated by assuming that the tensile and compressive forces across the plane of the notch consist only of tensile (or compressive) stresses equal to the yield strength all along the ligament, as before, plus the crack tip force. The load is calculated by requiring the net load and net moment applied to each half of the specimen to be nil. Once the load has been calculated, Eq. 8 is used to calculate J . The result for J_p , is:

$$J_p = Q_p (\sigma_y - \partial F / \partial a) \quad (6)$$

The result for the single-edge-notched specimen is:

$$J_p = \sigma_y Q_p \left[1 - f' + \frac{[2f + (1-2\alpha)(1-f')]}{\sqrt{1 + 2f(1-2\alpha) - 2\alpha(1-\alpha)}} \right] \quad (7)$$

where $f = F/\sigma_y TW$, $\alpha = a/w$, and $f' = \partial f / \partial \alpha$. The full expressions for the applied J value were formed by adding the linear elastic part to the plastic part.

Comparison of Results

The experimental load-displacement data for the specimen with the 30 mm notch are compared to calculated values from finite element analysis and the extended perfect plasticity theory in Fig. 7. The differences between experimental and calculated

values are attributed to strain-hardening effects not accurately accounted for in the calculations. Figure 8, in which load at a strain of 2 times yield is plotted against crack length, shows that the crack length dependences of both the experimental and the analytical results are well represented by the extended perfect plasticity theory.

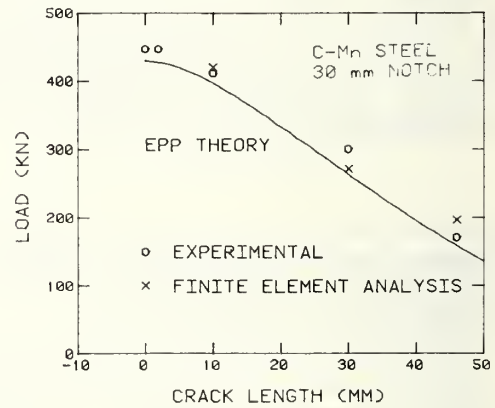
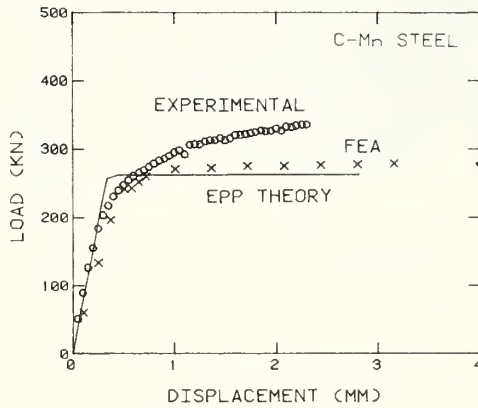


Fig. 7. Experimental, analytical, and theoretical results for the single-edge-notched specimen with the 30 mm notch; included are experimental, finite element analysis (FEA), and extended perfect plasticity (EPP) theory results.

Fig. 8. Load at a displacement of 2 times yield as a function of crack length; experimental, finite element analysis, and extended perfect plasticity (EPP) theory results are shown.

Figure 9 displays the contour integral, compliance, CTOD, finite element analysis and the extended perfect plasticity model results for the 30 mm notch plotted as functions of strain. The agreement among these different methods of determining the J-integral was not as good for the other notch lengths, because of the experimental problems noted above.

Practically all the measured and calculated J integral results had the same type of strain dependence. But the results of the theoretical models differ significantly in their dependence on crack length. This is shown in Fig. 10, which displays J as a function of crack length at a strain of 4 times the yield strain. Experimental results by the compliance and contour integral techniques, finite element analysis results, and the three theoretical models are plotted. This figure shows that the experimental results disagree with both the perfect plasticity and the uniform strain theories. The extended perfect plasticity theory predicts J values which lie between those of the uniform strain and perfect plasticity models, and best represents the experimental and analytical results. Similar conclusions were drawn from Fig. 11, in which the uniform strain, perfect plasticity, and extended perfect plasticity models are compared with one another and with finite element results for a center-notched-panel.

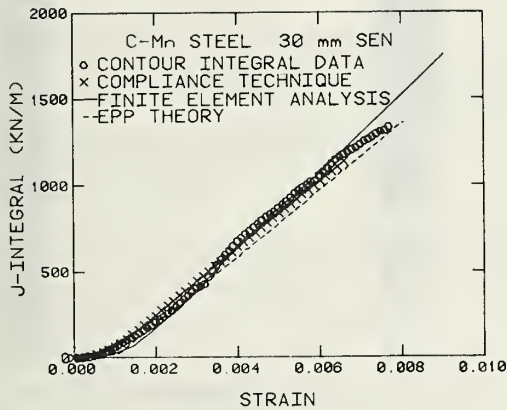


Fig. 9. Experimental, analytical, and theoretical results for single-edge-notched specimen with 30 mm notch; included are direct contour integral (CI), compliance technique (CT), finite element analysis (FEA), and extended perfect plasticity theory (EPP) results.

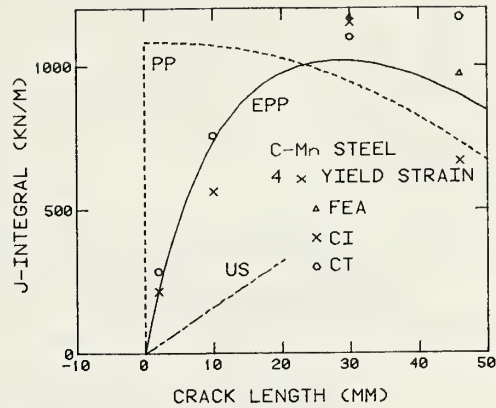


Fig. 10. Experimental, analytical, and theoretical results for the single-edge-notched specimens; included are direct contour integral (CI), compliance technique (CT), finite element analysis (FEA), uniform strain theory (US), perfect plasticity theory (PP) and extended perfect plasticity theory (EPP) results.

DISCUSSION

When this study was begun, it was hypothesized that the uniform strain model could be verified over a significant range of crack lengths. However, the experimental and analytical studies consistently produced J values several times those predicted by the uniform strain model; they were often in the neighborhood of the perfect plasticity result. But the perfect plasticity model was clearly unsatisfactory for short notch lengths. A physical interpretation of this result has been developed over the course of this study. This interpretation is that the uniform strain model holds only when plasticity conditions are such that plastic strains are spread over the whole length of the strained panel and are prevented from concentrating at the crack tip. A dramatic case of strain concentration at a crack tip is illustrated in Fig. 5. Slip bands at $\pm 45^\circ$ and 90° to the tensile axis emanated from the crack tip. Each increment of applied displacement contributed to the strain in the slip bands. Because the slip bands terminated at the crack tip, all the strain contributed to the opening of the crack. The photograph in Fig. 12 shows that the strains were not concentrated at the tip of the 10 mm notch as much as for the 2 mm notch, and the J values shown in Fig. 3 for strains between 0.002 and 0.003 are lower for the 10 mm notch.

It is concluded that the limiting cases for the behavior of J as a function of strain in tensile panels are provided by the uniform strain and perfect plasticity models. In the uniform strain model only limited strain concentration at the crack tip is allowed; in the perfect plasticity model all the plastic strain is concentrated at the crack tip. The extended perfect plasticity theory is intermediate between these two extremes.

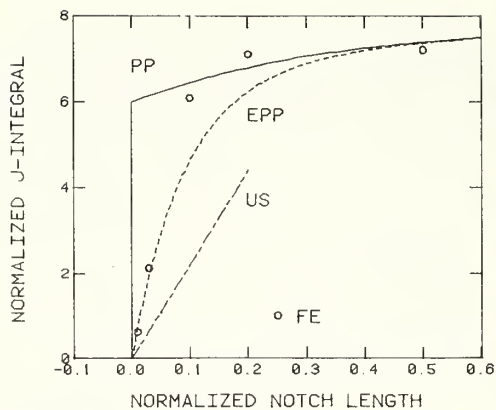


Fig. 11. Theoretical and analytical results for a center-notched-panel.

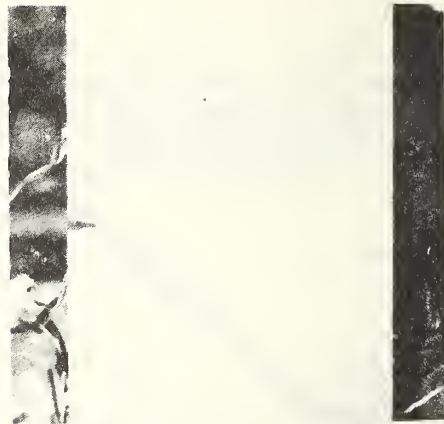


Fig. 12. Strain pattern, revealed by brittle lacquer, in ship steel specimen with 10 mm notch.

ACKNOWLEDGMENTS

The financial support of the U.S. Naval Sea Systems Command through J. P. Gudas, Project Monitor, and the technical assistance of J. W. Elmer, V. Hauptman and J. D. McColskey are gratefully acknowledged.

REFERENCES

- Begley, J. A., J. D. Landes, and W. K. Wilson (1974). An Estimation Model for the Application of the J-Integral. *Fracture Analysis*, ASTM STP 560, American Society for Testing and Materials, 155-169.
- Bucci, R. J., P. C. Paris, J. D. Landes, and J. R. Rice (1972). J Integral Estimation Procedures. *Fracture Toughness*, ASTM STP 514, American Society for Testing and Materials, 40-69.
- Burdekin, F. M., and D. E. W. Stone (1966). The Crack Opening Displacement Approach to Fracture Mechanics in Yielding Materials. *J. Strain Analysis*, 1, 145-153.
- Gifford, L. N. (1975). APES-Second Generation Two-Dimensional Fracture Mechanics and Stress Analysis by Finite Elements. David Taylor Naval Ship Research and Development Center, Bethesda, MD 20084, Report 4799.
- Gifford, L. N. (1978). J-Integral Analysis of a Compact J_{Ic} Specimen. David Taylor Naval Ship Research and Development Center, Bethesda, MD 20084, Report M-4.
- Hilton, P. D., and L. N. Gifford (1979). Evaluation of Some Crack Tip Finite Elements for Elastoplastic Fracture Analysis. David Taylor Naval Ship Research and Development Center, Bethesda, MD 20084, Structures Department Research and Development Report DTNSRDC-79/052.
- Hutchinson, J. W. (1968). Singular Behavior at the End of a Tensile Crack in a Hardening Material. *J. Mech. Phys. Solids*, 16, 13-31.
- Paris, P. C., H. Tada, A. Zahoor, and H. Ernst (1979). The Theory of the Tearing Mode of Elastic-Plastic Crack Growth. *Elastic Plastic Fracture*, ASTM STP 668, American Society for Testing and Materials, 5-36.
- Read, D. T. and H. I. McHenry (1980) Detailed Report on Strain Dependence of the J-Contour Integral. To be published.
- Rice, J. R., P. C. Paris, and J. G. Merkle (1973). Some Further Results of J-Integral Analysis and Estimates. *Progress in Flaw Growth and Fracture Toughness Testing*, ASTM STP 536, American Society for Testing and Materials, 231-245.
- Rice, J. R., and G. F. Rosengren (1968). Plane Strain Deformation Near a Crack Tip in a Power-Law Hardening Material. *J. Mech. Phys. Solids*, 16, 1-12.

